LOW-FREQUENCY FLUTE INSTABILITIES IN INTENSE NONNEUTRAL ELECTRON AND ION BEAMS

Han S. Uhm

and

Ronald C. Davidson

PFC/JA-79-19

LOW-FREQUENCY FLUTE INSTABILITIES IN INTENSE NONNEUTRAL ELECTRON AND ION BEAMS

Han S. Uhm
Naval Surface Weapons Center
White Oak, Silver Spring, Maryland 20910

and

Ronald C. Davidson*
Science Applications, Inc.
934 Pearl St., Boulder, Co., 80302

The stability properties for low-frequency flute perturbations in a relativistic nonneutral electron beam are investigated within the framework of the Vlasov-Maxwell equations. It is assumed that $\nu/\gamma_b << 1$, where ν is Budker's parameter and $\gamma_b mc^2$ is the characteristic electron energy. The analysis is carried out for the rigid-rotor equilibrium distribution function in which all electrons have the same value of energy in a frame rotating with angular velocity ω_b and the same value of axial canonical momentum. Strong instability is found for azimuthally symmetric perturbations ($\partial/\partial\theta = 0$) with radial mode number $n = 2$ and rotational frequency $\omega_b = 0.5\ \omega_{cb}$, where ω_{cb} is the electron cyclotron frequency. However, the instability can be easily stabilized by slightly detuning the rotational frequency from the value $\omega_b = 0.5\ \omega_{cb}$. The transverse stability properties of an intense ion beam in a quadrupole magnetic field are also investigated by analogy with the electron beam stability analysis, including the important influence of rotational effects on stability behavior. It is found that the rotational motion also plays an important role in determining the stability properties of intense ion beams.

---

* Permanent address: Plasma Fusion Center
Massachusetts Institute of Technology
Cambridge MA 02139

I. INTRODUCTION

In recent years, there have been numerous investigations of the equilibrium[1,2] and stability[3] properties of intense relativistic nonneutral electron beams, with emphasis on applications ranging from intense microwave generation[4] to collective ion acceleration.[5-7] In circumstances where the relativistic electron beam is propagating through a cylindrical conducting waveguide, various instabilities are possible. One of the most destructive instabilities that deteriorates the beam quality is associated with low-frequency flute perturbations. This paper examines stability properties for low-frequency flute perturbations about an intense nonneutral electron beam equilibrium. With straightforward modifications, the results of this paper can also be applied to the transverse instability[8,9] for an intense ion beam in a quadrupole magnetic field, which is particularly important in heavy-ion fusion applications.[10]

The analysis is carried out within the framework of the Vlasov-Maxwell equations for an infinitely long electron beam propagating parallel to a uniform magnetic field $B_0\hat{e}_z$ through a cylindrical conducting waveguide with radius R_c (Fig. 1). It is assumed that $\nu/\gamma_b \ll 1$, where ν and $\gamma_b mc^2$ are Budker's parameter and the characteristic electron energy, respectively, m is the electron rest mass and c is the speed of light in vacuo. Equilibrium and stability properties are calculated for the specific choice of equilibrium beam distribution function [Eq. (3)] in which all electrons have the same value of energy in a frame rotating with angular velocity ω_b, and the same value of axial canonical momentum.

Equilibrium properties are discussed in Sec. II, and the linearized Vlasov-Maxwell equations are investigated in Sec. III.

Stability properties for low-frequency perturbations characterized by

$$|\omega R_b| << \ell c$$

are investigated in Sec. IV, including the important influence of electron thermal Larmor radius effects on stability behavior. Here ω is the complex eigenfrequency, ℓ is the azimuthal harmonic number, and R_b is the beam radius. The analysis is carried out within the framework of the linearized Vlasov-Maxwell equations for a relativistic electron beam propagating parallel to a uniform axial magnetic field, assuming that all perturbed quantities are independent of axial coordinate ($\partial/\partial z=0$). The stability results in Sec. IV can be directly applied to the electron beam experiment at the University of Maryland.[11]

As an important generalization of the stability analysis developed in this paper, in Sec. V we investigate the influence of beam rotation on the transverse instability[8,9] for an intense ion beam in a quadrupole magnetic field, making use of the results obtained in Sec. IV. The transverse instability in an intense ion beam, originates from the influence of equilibrium self fields, and is particularly important in heavy-ion fusion applications.[10] Theoretical and experimental studies of this instability are currently being conducted at various locations.[9-14] In order to make the analysis tractable, we assume that the influence of the quadrupole field can be represented (approximately) by an effective axial vector potential as shown in previous analyses.[8]

II. EQUILIBRIUM PROPERTIES

The equilibrium configuration (Fig. 1) consists of a relativistic nonneutral electron beam propagating parallel to a uniform applied magnetic field $B_0\hat{e}_z$. Cylindrical polar coordinates (r,θ,z) are used, with z-axis along the axis of symmetry. The mean motion of the electron beam is in the axial and azimuthal directions, and the applied magnetic field provides radial confinement of the electrons. In equilibrium $(\partial/\partial t=0)$, the beam is assumed to be azimuthally symmetric $(\partial/\partial\theta=0)$, infinitely long, and axially uniform $(\partial/\partial z=0)$. The number of electrons per unit axial length (N_b) is defined by

$$N_b=2\pi\int_0^\infty dr\ r\ n_b^0(r)=\pi R_b^2 n_b^0(r=0)\ , \tag{1}$$

where $n_b^0(r)$ is the equilibrium density profile, and R_b is the characteristic beam radius. To make the analysis tractable, it is also assumed that

$$\frac{\nu}{\gamma_b}=\frac{N_b e^2}{mc^2}\frac{1}{\gamma_b}\ll 1\ , \tag{2}$$

where ν is Budker's parameter, c is the speed of light in <u>vacuo</u>, $\gamma_b mc^2$ is the characteristic electron energy, -e and m are the electron charge and rest mass, respectively. Equation (2) is equivalent to the paraxial approximation.

In this paper, we investigate the equilibrium and stability properties for a steady-state $(\partial/\partial t=0)$ beam distribution of the form

$$f_b^0(H,P_\theta,P_z)=\frac{\hat{n}_b}{2\pi\gamma_b m}\,\delta(H-\omega_b P_\theta-\hat{\gamma}mc^2)\,\delta(P_z-\gamma_b m\beta_b c)\ , \tag{3}$$

where the total energy,

$$H=(m^2c^4+c^2p_z^2)^{1/2}-e\phi_0(r)\ , \tag{4}$$

the canonical angular momentum,

$$P_\theta=(rp_\theta-eB_0r^2/2c) \ , \tag{5}$$

and the axial canonical momentum,

$$P_z=p_z-(e/c)A_0(r) \ , \tag{6}$$

are the three single-particle constants of the motion in the equilibrium fields. In Eqs. (3)-(6), $\underset{\sim}{p}=(p_r,p_\theta,p_z)$ is the mechanical momentum, $\hat{n}_b$ and $\hat{\gamma}$ are constants, γ_b is related to β_b by $\gamma_b=(1-\beta_b^2)^{-1/2}$, $A_0(r)$ is the axial component of vector potential for the equilibrium azimuthal self-magnetic field, and $\phi_0(r)$ is the equilibrium electrostatic potential. In defining the canonical angular momentum in Eq. (5), we have neglected the axial self magnetic field $B_z^s(r)$, which is consistent with Eq. (2).

The equilibrium self-field potentials are to be calculated self-consistently from the steady-state Maxwell equations. The equilibrium Poisson equation can be expressed as

$$\frac{1}{r}\frac{\partial}{\partial r}\,r\,\frac{\partial}{\partial r}\,\phi_0(r)=4\pi e n_b^0(r) \ , \tag{7}$$

where the electron density is defined by

$$n_b^0(r)=\int d^3p\ f_b^0(H,P_\theta,P_z) \ . \tag{8}$$

Furthermore, the z-component of the equilibrium $\nabla\times\underset{\sim}{B}$ Maxwell equation can be expressed as

$$\frac{1}{r}\frac{\partial}{\partial r}\,r\,\frac{\partial}{\partial r}\,A_0(r)=\frac{4\pi}{c}\,en_b^0(r)V_z^0(r) \ , \tag{9}$$

where the mean axial velocity is defined by

$$V_z^0(r)=\frac{\int d^3p\ v_z\ f_b^0(H,P_\theta,P_z)}{\int d^3p\ f_b^0(H,P_\theta,P_z)} \ , \tag{10}$$

and $v_z=p_z/[m(1+p_\perp^2/m^2c^2)^{1/2}]$ is the axial velocity of an electron.

Consistent with Eq. (2), the r-θ kinetic energy is assumed to be small in comparison with the rest mass energy. After some straightforward algebra, it follows that $H-\omega_b P_\theta$ can be approximated by[3]

$$H-\omega_b P_\theta=\gamma_b mc^2+\frac{p_\perp^2}{2\gamma_b m}+\frac{1}{2}\gamma_b m\Omega_b^2 r^2 \quad , \tag{11}$$

where $p_\perp$ and Ω_b are defined by

$$p_\perp^2=p_r^2+(p_\theta-\gamma_b m\omega_b r)^2 \quad , \tag{12}$$

$$\Omega_b^2=(\omega_b^+-\omega_b)(\omega_b-\omega_b^-)=\omega_b\omega_{cb}-\omega_b^2-\omega_{pb}^2/2\gamma_b^2 \quad . \tag{13}$$

In Eq. (13),

$$\omega_b^\pm=\frac{\omega_{cb}}{2}\left[1\pm\left(1-\frac{2\omega_{pb}^2}{\gamma_b^2\omega_{cb}^2}\right)^{1/2}\right] \quad , \tag{14}$$

denotes the fast (+) and slow (-) laminar rotation frequencies, $\omega_{cb}=eB_0/\gamma_b mc$ is the electron cyclotron frequency, and $\omega_{pb}^2=4\pi e^2\hat{n}_b/\gamma_b m$ is the electron plasma frequency-squared.

Substituting Eqs. (3) and (11) into Eq. (8), we find

$$n_b^0(r)=\begin{cases}\hat{n}_b \ , & 0\le r<R_b \ , \\ 0 \ , & R_b<r<R_c \ ,\end{cases} \tag{15}$$

where the beam radius R_b is defined by

$$R_b^2=2c^2(\hat{\gamma}-\gamma_b)/\gamma_b\Omega_b^2 \quad . \tag{16}$$

It is important to note that Eq. (10) can be approximated by

$$V_z^0(r)=\beta_b c \quad , \tag{17}$$

for $\nu/\gamma_b \ll 1$. Moreover, the mean azimuthal velocity of an electron fluid element is given by

$$V_\theta^0(r)=(\int d^3p\ v_\theta\ f_b^0)/(\int d^3p\ f_b^0)=\omega_b r\ , \tag{18}$$

for the rigid-rotor distribution in Eq. (3). Furthermore, it can be shown that the equilibrium pressure tensor in the plane perpendicular to z-axis is isotropic with perpendicular pressure $P_\perp^0(r)=n_b^0(r)T_\perp^0(r)$ given by

$$n_b^0(r)T_\perp^0(r)=2\pi\int_0^\infty dp_\perp p_\perp\int_{-\infty}^\infty dp_z\ \frac{p_r^2+(p_\theta-\gamma_b m\omega_b r)^2}{2\gamma_b m}\ f_b^0\ , \tag{19}$$

where $T_\perp^0(r)$ is the transverse temperature profile. Defining

$$\hat{T}_\perp=\frac{1}{2}\ \gamma_b m\Omega_b^2R_b^2=\frac{1}{2}\ \gamma_b m\omega_{cb}^2r_L^2 \tag{20}$$

and substituting Eq. (3) into Eq. (19) gives

$$T_\perp^0(r)=\hat{T}_\perp(1-r^2/R_b^2) \tag{21}$$

for $0 < r < R_b$. In Eq. (20), r_L is the characteristic thermal Larmor radius of the beam electrons.

Making use of Eq. (20) to eliminate Ω_b in Eq. (13) in favor of r_L, we obtain

$$\omega_b=\hat{\omega}_b^\pm=\frac{1}{2}\ \omega_{cb}\left\{1\pm\left[1-\frac{2\omega_{pb}^2}{\gamma_b^2\omega_{cb}^2}-\left(\frac{2r_L}{R_b}\right)^2\right]^{1/2}\right\}\ , \tag{22}$$

which relates the rotational frequency ω_b to the Larmor radius r_L. The two signs (±) again represent fast (+) and slow (-) rotational equilibria. In order for the equilibrium to exist, the Larmor radius r_L in Eq. (22) is restricted to the range

$$\left(\frac{2r_L}{R_b}\right)^2\leq 1-\frac{2\omega_{pb}^2}{\gamma_b^2\omega_{cb}^2}\ , \tag{23}$$

which is plotted in Fig. 2. Figure 3 shows a plot of rotation frequency ω_b [Eq. (22)] versus $2\omega_{pb}^2/\gamma_b^2\omega_{cb}^2+(2r_L/R_b)^2$. We note from Fig. 3 that the $\hat{\omega}_b^\pm$

curves converge to the common point $\hat{\omega}_b^{\pm}=0.5\ \omega_{cb}$ for a value of beam density satisfying $2\omega_{pb}^2/\gamma_b^2\omega_{cb}^2+(2r_L/R_b)^2=1$. We also note from Fig. 3 that no equilibrium solutions exist in the region where $2\omega_{pb}^2/\gamma_b^2\omega_{cb}^2+(2r_L/R_b)^2 > 1$. Under normal circumstances, the electron beam is in a slow rotational equilibrium characterized by $\omega_b=\hat{\omega}_b^-$ where

$$\hat{\omega}_b^- = \frac{1}{2}\ \omega_{cb} \left\{1-\left[1- \frac{2\omega_{pb}^2}{\gamma_b^2\omega_{cb}^2} - \left(\frac{2r_L}{R_b}\right)^2\right]^{1/2}\right\} \quad . \tag{24}$$

III. LINEARIZED VLASOV-MAXWELL EQUATIONS

In this section, we formally integrate the linearized Vlasov equations for a relativistic electron beam. The linearized Vlasov equation for the perturbed distribution function $\delta f_b(\underset{\sim}{x},\underset{\sim}{p},t)$ can be expressed as

$$\left\{\frac{\partial}{\partial t}+\underset{\sim}{v}\cdot\frac{\partial}{\partial \underset{\sim}{x}}-e\left[\underset{\sim}{E}_0^s(\underset{\sim}{x})+\frac{\underset{\sim}{v}\times\underset{\sim}{B}_0(\underset{\sim}{x})}{c}\right]\cdot\frac{\partial}{\partial \underset{\sim}{p}}\right\}\ \delta f_b(\underset{\sim}{x},\underset{\sim}{p},t)$$

$$=e\left[\delta\underset{\sim}{E}(\underset{\sim}{x},t)+\frac{\underset{\sim}{v}\times\delta\underset{\sim}{B}(\underset{\sim}{x},t)}{c}\right]\cdot\frac{\partial}{\partial \underset{\sim}{p}}\ f_b^0(H,P_\theta,P_z) \tag{25}$$

where $\underset{\sim}{E}_0^s(\underset{\sim}{x})=-(\partial/\partial r)\phi_0(r)\hat{\underset{\sim}{e}}_r$ is the equilibrium self-electric field, $\underset{\sim}{B}_0(\underset{\sim}{x})=B_0\hat{\underset{\sim}{e}}_z+B_{0\theta}^s(r)\hat{\underset{\sim}{e}}_\theta$ is the total equilibrium magnetic field, $\delta\underset{\sim}{E}(\underset{\sim}{x},t)$ and $\delta\underset{\sim}{B}(\underset{\sim}{x},t)$ are the perturbed electric and magnetic fields, and $(\hat{\underset{\sim}{e}}_r,\hat{\underset{\sim}{e}}_\theta,\hat{\underset{\sim}{e}}_z)$ are cylindrical polar unit vectors. We substitute $\delta\underset{\sim}{E}(\underset{\sim}{x},t)=\hat{\underset{\sim}{E}}(\underset{\sim}{x})\exp(-i\omega t)$ and $\delta\underset{\sim}{B}(\underset{\sim}{x},t)=\hat{\underset{\sim}{B}}(\underset{\sim}{x})\exp(-i\omega t)$ on the right-hand side of Eq. (25), and integrate from $t'=-\infty$ to $t'=t$, using the method of characteristics and assuming $\mathrm{Im}\omega > 0$. Neglecting initial perturbations, we find

$$\hat{f}_b(\underset{\sim}{x},\underset{\sim}{p})=e\int_{-\infty}^{0}d\tau\exp(-i\omega\tau)\ \left\{\hat{\underset{\sim}{E}}(\underset{\sim}{x}')+\frac{1}{c}\left[\underset{\sim}{v}'\times\hat{\underset{\sim}{B}}(\underset{\sim}{x}')\right]\right\}\cdot\frac{\partial}{\partial \underset{\sim}{p}'}\ f_b^0\ , \tag{26}$$

where $\tau=t'-t$, $\delta f_b(\underset{\sim}{x},\underset{\sim}{p},t)=\hat{f}_b(\underset{\sim}{x},\underset{\sim}{p})\exp(-i\omega t)$, and the particle trajectories $\underset{\sim}{x}'(t')$ and $\underset{\sim}{v}'(t')$ satisfy the "initial" conditions $\underset{\sim}{x}'(\tau=0)=\underset{\sim}{x}$ and $\underset{\sim}{v}'(\tau=0)=\underset{\sim}{v}$.

The Maxwell equations for the perturbed field amplitudes can be expressed as

$$\nabla\cdot\hat{\underset{\sim}{E}}(\underset{\sim}{x})=4\pi\hat{\rho}(\underset{\sim}{x})$$

$$\nabla\times\hat{\underset{\sim}{E}}(\underset{\sim}{x})=i(\omega/c)\hat{\underset{\sim}{B}}(\underset{\sim}{x})$$

$$\nabla\times\hat{\underset{\sim}{B}}(\underset{\sim}{x})=(4\pi/c)\hat{\underset{\sim}{J}}(\underset{\sim}{x})-i(\omega/c)\hat{\underset{\sim}{E}}(\underset{\sim}{x})\ , \tag{27}$$

where the perturbed charge and current densities are defined by

$$\hat{\rho}(\underset{\sim}{x})=-e\int d^3p\ \hat{f}_b(\underset{\sim}{x},\underset{\sim}{p}) \tag{28}$$

and

$$\hat{\underset{\sim}{J}}(\underset{\sim}{x})=-e\int d^3p\ \underset{\sim}{v}\ \hat{f}_b(\underset{\sim}{x},\underset{\sim}{p})\ , \tag{29}$$

respectively. Here $\underset{\sim}{v}=\underset{\sim}{p}/[m(1+\underset{\sim}{p}^2/m^2c^2)^{1/2}]$ is the particle velocity.

In order to carry out the time integration in Eq. (26), it is useful to introduce the polar momentum variables $(p_\perp,\phi)$ in the rotating frame defined by

$$\begin{aligned} p_x+\gamma_b m\omega_b y&=p_\perp\cos\phi\ , \\ p_y-\gamma_b m\omega_b x&=p_\perp\sin\phi\ , \end{aligned} \tag{30}$$

where $p_\perp^2=p_r^2+(p_\theta-\gamma_b m\omega_b r)^2$. Note also that the Cartesian coordinates (x,y) are related to the polar coordinates (r,θ) by $x=r\cos\theta$, and $y=r\sin\theta$. In this context, the perpendicular electron trajectories can be expressed as[3]

$$\begin{aligned} x'(\tau)=\frac{1}{\omega_b^+-\omega_b^-}\Bigg\{&\frac{p_\perp}{\gamma_b m}\left[\sin(\phi+\omega_b^+\tau)-\sin(\phi+\omega_b^-\tau)\right] \\ &+r(\omega_b-\omega_b^-)\cos(\theta+\omega_b^+\tau)-r(\omega_b-\omega_b^+)\cos(\theta+\omega_b^-\tau)\Bigg\}\ , \\ y'(\tau)=\frac{1}{\omega_b^+-\omega_b^-}\Bigg\{&\frac{p_\perp}{\gamma_b m}\left[\cos(\phi+\omega_b^-\tau)-\cos(\phi+\omega_b^+\tau)\right] \\ &+r(\omega_b-\omega_b^-)\sin(\theta+\omega_b^+\tau)-r(\omega_b-\omega_b^+)\sin(\theta+\omega_b^-\tau)\Bigg\}\ , \end{aligned} \tag{31}$$

where the frequencies $\omega_b^\pm$ are defined in Eq. (14).

IV. STABILITY ANALYSIS

Stability properties for long axial wavelength perturbations characterized by

$$k_z=0 \tag{32}$$

are investigated in this section, including the important influence of electron thermal Larmor radius effects on stability behavior. Here, k_z is the axial wavenumber. The stability results obtained in this section can be directly applied to the electron beam experiment at University of Maryland.[11] In order to make the stability analysis tractable, we assume

$$|\omega R_b| << \ell c \ , \tag{33}$$

where ω is the complex eigenfrequency, and ℓ is the azimuthal harmonic number.

Fourier decomposing the perturbed field amplitudes according to

$$\hat{\phi}(\underset{\sim}{x})=\hat{\phi}(r)\exp(i\ell\theta) \ ,$$

and making use of Eqs. (32) and (33), it is straightforward to show that the Maxwell equations in Eq. (27) can be combined to give

$$\left(\frac{1}{r}\frac{\partial}{\partial r}\, r\, \frac{\partial}{\partial r} - \frac{\ell^2}{r^2}\right)\psi(r)=-4\pi\left[\hat{\rho}(r)-\frac{\beta_b}{c}\,\hat{J}_z(r)\right] \ , \tag{34}$$

where the effective perturbed potential $\psi(r)$ is defined by

$$\psi(r)=(ir/\ell)[\hat{E}_\theta(r)+\beta_b\hat{B}_r(r)] \ . \tag{35}$$

From Eq. (2), the axial component of perturbed current density $\hat{J}_z(r)$ is related to perturbed charge density $\hat{\rho}(r)$ by $\hat{J}_z(r)=\beta_b c\hat{\rho}(r)$. Therefore, Eq. (34) can be further simplified to give

$$\left(\frac{1}{r}\frac{\partial}{\partial r}\, r\, \frac{\partial}{\partial r} - \frac{\ell^2}{r^2}\right)\psi(r) = -\frac{4\pi}{\gamma_b^2}\,\hat{\rho}(r) \quad . \tag{36}$$

To obtain the perturbed charge density $\hat{\rho}(r)$ in Eq. (36), it is necessary to calculate the perturbed distribution function $\hat{f}_b$ in Eq. (26). After some straightforward algebra that makes use of the definition in Eq. (35), we obtain

$$\left(\frac{1}{r}\frac{\partial}{\partial r}\, r\, \frac{\partial}{\partial r} - \frac{\ell^2}{r^2}\right)\psi(r) = -\frac{4\pi e^2 m}{\gamma_b}\int d^3p\, \frac{1}{p_\perp}\frac{\partial f_b^0}{\partial p_\perp}\left(\psi(r) + i(\omega-\ell\omega_b)\int_{-\infty}^{0} d\tau\psi(r')\exp\{i[\ell(\theta'-\theta)-\omega\tau]\}\right) \quad . \tag{37}$$

In obtaining Eq. (37), we have neglected terms proportional to $\partial f_b^0/\partial P_z$, since the corrections associated with these terms are of order v/γ_b ($<<1$) or smaller. Moreover, the term proportional to $(v_r/c)\hat{B}_z$ in Eq. (26) has also been neglected, because the r-θ kinetic energy is assumed to be small in comparison with $\gamma_b mc^2$. Substituting Eq. (3) into Eq. (37), and carrying out the integration over p_z give

$$\left(\frac{1}{r}\frac{\partial}{\partial r}\, r\, \frac{\partial}{\partial r} - \frac{\ell^2}{r^2}\right)\psi(r) = -\frac{8\pi e^2 m\hat{n}_b}{\gamma_b}\int_0^\infty dp_\perp^2\, \frac{d}{dp_\perp^2}\,\delta[p_\perp^2-\gamma_b^2 m^2\Omega_b^2(R_b^2-r^2)] \times[\psi(r)+(\omega-\ell\omega_b)\hat{I}] \quad , \tag{38}$$

where the orbit integral $\hat{I}$ is defined by

$$\hat{I} = i\int_0^{2\pi}\frac{d\phi}{2\pi}\int_{-\infty}^{0} d\tau\psi(r')\exp\{i[\ell(\theta'-\theta)-\omega\tau]\} \quad . \tag{39}$$

A highly simplified nonrelativistic version of Eq. (38) was first obtained by Gluckstern,[8] making use of Kapchinsky-Vladimirsky distribution,[15] where the beam rotational frequency ω_b is assumed to be independent of the electron thermal Larmor radius. However, for the rigid-rotor equilibrium distribution considered here, the rotational frequency ω_b is related to the thermal Larmor radius r_L through the equilibrium constraint in Eq. (24),

and plays an important role in determining stability behavior. Carrying out the integration over $p_\perp^2$ in Eq. (38), we obtain

$$\left(\frac{1}{r}\frac{\partial}{\partial r}\, r\, \frac{\partial}{\partial r} - \frac{\ell^2}{r^2}\right)\psi(r) = \frac{\omega_{pb}^2\,\delta(r-R_b)}{\gamma_b^2\Omega_b^2 R_b}\,[\psi(R_b)+(\omega-\ell\omega_b)\hat{I}(R_b)] + \frac{8\pi e^2 m\hat{n}_b}{\gamma_b}\,(\omega-\ell\omega_b)\Theta(R_b-r)\left(\frac{d}{dp_\perp^2}\,\hat{I}\right)_{p_\perp^2=p_0^2}, \tag{40}$$

where the Heaviside step function $\Theta(x)$ is defined by

$$\Theta(x)=\begin{cases} 0\,, & x<0 \\ 1\,, & x>0 \end{cases} \tag{41}$$

and $p_0^2 \equiv \gamma_b^2 m^2 \Omega_b^2 (R_b^2 - r^2)$. In general, the perturbed potential $\psi(r)$ that solves Eq. (40) can be expressed as

$$\psi(r)=Ar^\ell\left\{\sum_{j=0}^{n} a_j(\omega)(r/R_b)^{2j}\right\}, \tag{42}$$

for $0 \le r \le R_b$. In Eq. (42), $a_0=1$, A is a constant, and the coefficients $a_j(\omega)$ are generally a function of the complex eigenfrequency ω, with $a_j(\omega)$ determined self-consistently for each class of solutions to Eq. (40). In the subsequent analysis, we refer to n as the radial mode number. The stability properties for specific values of radial mode number n are investigated in the remainder of this section.

A. Surface Perturbations with n=0

As a reference case for the subsequent analysis, we first consider the case where n=0, i.e.,

$$\psi(r)=Ar^\ell\,, \quad 0 \le r \le R_b\,. \tag{43}$$

Substituting Eq. (43) into Eq. (39), and making use of the orbits in Eq. (31) and the identity $r\exp(i\theta)=x+iy$, we obtain[3]

$$\hat{I}=\frac{i\psi(r)}{(\omega_b^+-\omega_b^-)^{\ell}}\int_{-\infty}^{0}d\tau\exp(-i\omega\tau)[(\omega_b-\omega_b^-)\exp(i\omega_b^+\tau)-(\omega_b-\omega_b^+)\exp(i\omega_b^-\tau)]^{\ell} . \tag{44}$$

Since the orbit integral $\hat{I}$ in Eq. (44) is independent of $p_\perp^2$, the second term on the right-hand side of Eq. (40) vanishes in this particular case, and the perturbed charge density is zero except at the surface of the beam [the term proportional to $\delta(r-R_b)$ in Eq. (40)]. We therefore refer to the corresponding solution to Eq. (40) as a surface-wave perturbation. From Eqs. (40) and (44), we note that the eigenfunction $\psi(r)$ satisfies the vacuum Poisson equation $r^{-1}(\partial/\partial r)[r\partial\psi/\partial r]-(\ell^2/r^2)\psi=0$, except at $r=R_b$. Therefore the solution to Eq. (40) can be expressed as

$$\psi(r)=Ar^{\ell}\begin{cases}1 , & 0\le r<R_b ,\\ (1-R_c^{2\ell}/r^{2\ell})/(1-R_c^{2\ell}/R_b^{2\ell}) , & R_b<r\le R_c ,\end{cases} \tag{45}$$

where R_c is the radius of outer conductor (Fig. 1).

The dispersion relation that determines the complex eigenfrequency ω is obtained by multiplying Eq. (40) by r and integrating from $R_b(1-\varepsilon)$ to $R_b(1+\varepsilon)$ with $\varepsilon\to 0_+$. This gives the dispersion relation

$$D_0(\omega)=\frac{2}{1-(R_b/R_c)^{2\ell}}-\frac{\omega_{pb}^2R_b^2}{\ell\omega_{cb}^2r_L^2}\Gamma_{\ell}(\omega)=0 , \tag{46}$$

where

$$\Gamma_{\ell}(\omega)=-1+\left(\frac{\omega_b^+-\omega_b}{\omega_b^+-\omega_b^-}\right)^{\ell}\sum_{m=0}^{\ell}\frac{\ell!}{m!(\ell-m)!}\frac{\omega-\ell\omega_b}{\omega-\ell\omega_b^--m(\omega_b^+-\omega_b^-)}\left(\frac{\omega_b-\omega_b^-}{\omega_b^+-\omega_b}\right)^{m}, \tag{47}$$

and use has been made of Eqs. (20), (44), and (45). After a careful examination of Eqs. (46) and (47), we find that all solutions to Eq. (46) have $\mathrm{Im}\omega=0$ provided ω_b lies in the range $\omega_b^-<\omega_b<\omega_b^+$, which is the necessary condition for existence of the equilibrium [Eq. (13)]. In this context, we conclude that the n=0 surface perturbation described by Eqs. (45)

and (46) does not exhibit instability for a nonneutral electron beam with only one species of particles (beam electrons).

B. n=1 Body-Wave Perturbations

As a first example of body-wave perturbations, we consider the n=1 eigenfunction given by

$$\psi(r)=Ar^{\ell}[1+a_1(\omega)(r/R_b)^2] \ , \tag{48}$$

for $0 \leq r \leq R_b$. In order to evaluate the orbit integral $\hat{I}$ in Eq. (39), we express

$$\begin{aligned}[r'\exp(i\theta')]^{\ell} &= [x'(\tau)+y'(\tau)]^{\ell} \\ &= \frac{1}{(\omega_b^+-\omega_b^-)^{\ell}}\left[i\alpha_1(\tau)\frac{p_\perp}{\gamma_b m}\exp(i\phi)+r\alpha_2(\tau)\exp(i\theta)\right]^{\ell} \ ,\end{aligned} \tag{49}$$

where

$$\begin{aligned}\alpha_1(\tau) &= \exp(i\omega_b^-\tau)-\exp(i\omega_b^+\tau) \ , \\ \alpha_2(\tau) &= (\omega_b-\omega_b^-)\exp(i\omega_b^+\tau)-(\omega_b-\omega_b^+)\exp(i\omega_b^-\tau) \ .\end{aligned} \tag{50}$$

Moreover, it is straightforward to show from Eq. (31) that

$$\begin{aligned}[(\omega_b^+-\omega_b^-)r']^2 &= \frac{2p_\perp^2}{\gamma_b^2 m^2}[1-\cos(\omega_b^+-\omega_b^-)\tau]+r^2[(\omega_b-\omega_b^-)^2+(\omega_b-\omega_b^+)^2] \\ &+2r^2(\omega_b^+-\omega_b)(\omega_b-\omega_b^-)\cos(\omega_b^+-\omega_b^-)\tau+\frac{2p_\perp}{\gamma_b m}r(\omega_b-\omega_b^-)\{\sin(\phi-\theta) \\ &+\sin[(\omega_b^+-\omega_b^-)\tau-(\phi-\theta)]\}+\frac{2p_\perp}{\gamma_b m}r(\omega_b-\omega_b^+)\{\sin(\phi-\theta) \\ &-\sin[(\omega_b^+-\omega_b^-)\tau+(\phi-\theta)]\} \ .\end{aligned} \tag{51}$$

Making use of Eqs. (49)-(51), we find that the orbit integral $\hat{I}$

can be expressed as

$$\hat{I}= \frac{i\psi(r)}{(\omega_b^+-\omega_b^-)^\ell}\int_{-\infty}^{0} d\tau \exp\{-i\omega\tau\}\alpha_2^\ell(\tau) - \frac{2Ar^\ell a_1(\omega)}{(\omega_b^+-\omega_b^-)^2(\omega-\ell\omega_b)}\left[(r/R_b)^2\Omega_b^2\chi_1(\omega)-\frac{p_\perp^2}{\gamma_b^2 m^2 R_b^2}\chi_2(\omega)\right], \tag{52}$$

where

$$\chi_1(\omega)= \frac{i(\omega-\ell\omega_b)}{(\omega_b^+-\omega_b^-)^\ell}\int_{-\infty}^{0} d\tau \exp\{-i\omega\tau\}\alpha_2^\ell(\tau)[1-\cos\{(\omega_b^+-\omega_b^-)\tau\}],$$

$$\chi_2(\omega)=\chi_1(\omega)+\frac{i\ell(\omega-\ell\omega_b)}{2(\omega_b^+-\omega_b^-)^\ell}\int_{-\infty}^{0} d\tau \exp\{-i\omega\tau\}\alpha_2^{\ell-1}(\tau)\alpha_1(\tau) \tag{53}$$

$$\times\left\{(\omega_b-\omega_b^-)[-1+\exp\{i(\omega_b^+-\omega_b^-)\tau\}]+(\omega_b-\omega_b^+)[-1+\exp\{-i(\omega_b^+-\omega_b^-)\tau\}]\right\}.$$

Note that the first term on the right-hand side of Eq. (52) is identical to Eq. (44). Substituting Eq. (52) into Eq. (40) and making use of the definition of $\Gamma_\ell(\omega)$ in Eq. (47) gives the eigenvalue equation

$$\left(\frac{1}{r}\frac{\partial}{\partial r}\,r\,\frac{\partial}{\partial r}-\frac{\ell^2}{r^2}\right)\psi(r)=-\frac{\omega_{pb}^2\delta(r-R_b)}{\gamma_b^2 R_b}\left[\frac{\psi(R_b)}{\Omega_b^2}\Gamma_\ell(\omega) + \frac{2AR_b^\ell a_1}{(\omega_b^+-\omega_b^-)^2}\chi_1(\omega)\right]+\frac{4\omega_{pb}^2 Ar^\ell a_1\chi_2(\omega)}{\gamma_b^2(\omega_b^+-\omega_b^-)^2R_b^2}\Theta(R_b-r), \tag{54}$$

where $\Theta(x)$ is Heaviside step function.

The eigenfunction $\psi(r)$ for n=1 and $\ell\neq 0$ can be expressed as

$$\psi(r)=Ar^\ell\begin{cases}1+a_1(r/R_b)^2, & 0\le r<R_b,\\ (1+a_1)(1-R_c^{2\ell}/r^{2\ell})/(1-R_c^{2\ell}/R_b^{2\ell}), & R_b<r<R_c,\end{cases} \tag{55}$$

where R_c is the radius of the conducting wall. Equation (54) can be solved inside the beam ($0\le r<R_b$) by substituting Eq. (55) into Eq. (54). Moreover, we multiply Eq. (54) by r and integrate from $R_b(1-\varepsilon)$ to $R_b(1+\varepsilon)$ with $\varepsilon\to 0_+$. After some straightforward algebraic manipulation, we obtain

$$\begin{pmatrix} \frac{1}{2}\,\ell D_0(\omega) , & 1-\dfrac{\omega_{pb}^2 \chi_1(\omega)}{\gamma_b^2(\omega_b^+-\omega_b^-)^2} \\ 0 , & D_1(\omega)-1 \end{pmatrix} \begin{pmatrix} \psi(R_b) \\ Aa_1 R_b^{\ell} \end{pmatrix} = 0 , \tag{56}$$

where $\psi(R_b)=A(1+a_1)R_b^{\ell}$,

$$D_1(\omega)=\frac{\omega_{pb}^2 \chi_2(\omega)}{(\ell+1)\gamma_b^2(\omega_b^+-\omega_b^-)^2} , \tag{57}$$

and $D_0(\omega)$ is defined in Eq. (46). Evidently, from Eq. (56), the dispersion relation can be expressed as

$$D_0(\omega)[D_1(\omega)-1]=0 ,$$

where $D_0(\omega)=0$ corresponds to the dispersion relation for (stable) surface-wave perturbations investigated in the previous section, and

$$D_1(\omega)=\frac{\omega_{pb}^2 \chi_2(\omega)}{(\ell+1)\gamma_b^2(\omega_b^+-\omega_b^-)^2}=1 , \tag{58}$$

corresponds to the dispersion relation for n=1 body-wave perturbations. In order to complete the stability analysis, it is necessary to express a_1 in terms of the eigenfrequency ω. After some straightforward algebra, we obtain

$$[a_1(\omega)]^{-1}=-1-2\left(1-\frac{\omega_{pb}^2 \chi_1(\omega)}{\gamma_b^2(\omega_b^+-\omega_b^-)^2}\right)\Big/\ell D_0(\omega) \tag{59}$$

for azimuthally asymmetric perturbations ($\ell\neq 0$).

For azimuthally symmetric perturbations ($\ell=0$), the eigenfunction $\psi(r)$ can be expressed as

$$\psi(r)=A\begin{cases} 1+a_1(r/R_b)^2 , & 0 \le r < R_b , \\ (1+a_1)\ell n(r/R_c)/\ell n(R_b/R_c), & R_b < r \le R_c . \end{cases} \tag{60}$$

Following similar steps to those used in the derivation of Eq. (59),

we obtain

$$\frac{1}{a_1}+1 \;=2\left(1-\frac{\omega_{pb}^2\chi_1(\omega)}{\gamma_b^2(\omega_b^+-\omega_b^-)^2}\right)\ln(R_b/R_c)\ .$$

From Eq. (53) we note that $\chi_1=\chi_2$ for $\ell=0$. Therefore, for $\ell=0$, we obtain

$$a_1(\omega)=-1\ .$$

(a) Perturbations with $(\ell,n)=(0,1)$. For $\ell=0$, the function $\chi_2(\omega)$ [Eq. (53)] is given by

$$\chi_2(\omega)=\frac{(\omega_b^+-\omega_b^-)^2}{\omega^2-(\omega_b^+-\omega_b^-)^2}\ . \tag{61}$$

Substituting Eq. (61) into Eq. (58) and making use of Eq. (14), we obtain the dispersion relation

$$\omega^2=\omega_{cb}^2-\omega_{pb}^2/\gamma_b^2 \tag{62}$$

for $\ell=0$ and $n=1$. It is straightforward to show from the equilibrium constraint in Eq. (23) that the right-hand side of Eq. (62) is always positive. We therefore conclude that perturbations with $(\ell,n)=(0,1)$ do not exhibit instability for any allowed value of thermal Larmor radius r_L.

(b) Perturbations with $(\ell,n)=(1,1)$. After some straightforward algebra for $(\ell,n)=(1,1)$, we obtain from Eq. (53)

$$\chi_2(\omega)=\left(\frac{\omega-\omega_b}{\omega_b^+-\omega_b^-}\right)\left\{\frac{\omega_b-\omega_b^-}{\omega-2\omega_b^++\omega_b^-}+\frac{\omega_b^++2\omega_b^--3\omega_b}{\omega-\omega_b^+}\right.$$
$$\left.+\frac{3\omega_b-2\omega_b^+-\omega_b^-}{\omega-\omega_b^-}+\frac{\omega_b^+-\omega_b}{\omega-2\omega_b^-+\omega_b^+}\right\}\ . \tag{63}$$

Substituting Eq. (63) into Eq. (55) gives the complete dispersion relation for perturbations with mode numbers $(\ell,n)=(1,1)$. Note that the dispersion relation $D_1(\omega)=1$ in Eq. (58), when combined with Eq. (63), is a fourth-order polynomial equation for the eigenfrequency ω. In order to investigate

stability properties from this dispersion relation, we plot the function $D_1(\omega)$ [Eq. (57)] versus real ω in Fig. 4 for the three ranges of ω_b satisfying (a) $\omega_b^+ + 2\omega_b^- > 3\omega_b$, (b) $2\omega_b^+ + \omega_b^- > 3\omega_b > \omega_b^+ + 2\omega_b^-$, and (c) $3\omega_b > 2\omega_b^+ + \omega_b^-$. The required roots are found from the intersection of the $D_1=1$ horizontal straight line with the $D_1(\omega)$ curves. Evidently, it follows from Fig. 4 that all four solutions to $D_1(\omega)=1$ correspond to real eigenfrequency ω. That is, there is no instability for mode numbers $(\ell,n)=(1,1)$.

(c) Perturbations with $(\ell,n)=(2,1)$. After some tedious algebraic manipulation, $\chi_2(\omega)$ [Eq. (53)] can be expressed as

$$\chi_2(\omega) = \frac{3(\omega-2\omega_b)}{2(\omega_b^+-\omega_b^-)^2}\left\{\frac{(\omega_b-\omega_b^-)^2}{\omega-3\omega_b^+ +\omega_b^-} + 2(\omega_b^+ +\omega_b^- -2\omega_b)\left(\frac{\omega_b-\omega_b^-}{\omega-2\omega_b^+} - \frac{\omega_b^+-\omega_b}{\omega-2\omega_b^-}\right)\right.$$
$$\left. + \frac{(2\omega_b-\omega_b^- -\omega_b^+)^2 - 2(\omega_b-\omega_b^-)(\omega_b^+-\omega_b)}{\omega-\omega_b^+-\omega_b^-} + \frac{(\omega_b^+-\omega_b)^2}{\omega-3\omega_b^- +\omega_b^+}\right\}, \qquad (64)$$

for perturbations with $(\ell,n)=(2,1)$. The dispersion relation, which is obtained by substituting Eq. (64) into Eq. (55), has been investigated for r_L/R_b in the range $0 \leq r_L/R_b < 0.5$, and values of the plasma frequency ω_{pb} satisfying Eq. (23). The numerical analysis of this dispersion relation indicates that perturbations with $(\ell,n)=(2,1)$ do not exhibit instability for the entire allowable range of r_L/R_b and ω_{pb}. Investigation of stability properties for higher ℓ values is considerably more complicated. However, the present stability analysis can be extended in a relatively straightforward manner to perturbations with azimuthal harmonic number $\ell \geq 3$.

C. n=2 Body-Wave Perturbations

As a second example of body-wave perturbations, we consider the n=2 eigenfunction

$$\psi(r) = Ar^{\ell}[1+a_1(r/R_b)^2 + a_2(r/R_b)^4], \qquad (65)$$

for $0 \leq r \leq R_b$. In order to illustrate stability properties for n=2,

we consider azimuthally symmetric ($\ell=0$) breathing mode perturbations in the remainder of this section. Substituting Eq. (65) into Eq. (39) and carring out some tedious algebraic manipulations that make use of Eq. (51), we determine that the orbit integral $\hat{I}$ satisfies

$$[(\omega_b^+-\omega_b^-)^2-\omega^2][\psi(r)+\omega\hat{I}]=2Aa_1\left(\Omega_b^2\frac{r^2}{R_b^2}-\frac{p_\perp^2}{\gamma_b^2m^2R_b^2}\right)$$
$$+Aa_2\left\{\frac{24p_\perp^2}{\gamma_b^2m^2R_b^2}\frac{(p_\perp^2/\gamma_b^2m^2R_b^2)-4\Omega_b^2(r/R_b)^2}{\omega^2-4(\omega_b^+-\omega_b^-)^2}-\frac{8p_\perp^2}{\gamma_b^2m^2R_b^2}\left(\frac{r}{R_b}\right)^2\right.$$
$$\left.+4\Omega_b^2\left(\frac{r}{R_b}\right)^2\left[1+\frac{6\Omega_b^2}{\omega^2-4(\omega_b^+-\omega_b^-)^2}\right]\right\}\quad , \tag{66}$$

for azimuthally symmetric perturbations ($\ell=0$). In Eq. (66), $\Omega_b^2=(\omega_b^+-\omega_b)\times(\omega_b-\omega_b^-)$ is defined in Eq. (13).

The eigenvalue equation can be determined by substituting Eq. (66) into Eq. (40). This gives

$$\frac{1}{r}\frac{\partial}{\partial r}\,r\,\frac{\partial}{\partial r}\,\psi=-\frac{2A\omega_{pb}^2\delta(r-R_b)}{\gamma_b^2R_b[\omega^2-(\omega_b^+-\omega_b^-)^2]}\left\{a_1+2a_2\left[1+\frac{6\Omega_b^2}{\omega^2-4(\omega_b^+-\omega_b^-)^2}\right]\right\}$$
$$+\frac{4A\omega_{pb}^2\Theta(R_b-r)}{\gamma_b^2R_b^2[\omega^2-(\omega_b^+-\omega_b^-)^2]}\left\{a_1-\frac{24a_2\Omega_b^2(1-3r^2/R_b^2)}{\omega^2-4(\omega_b^+-\omega_b^-)^2}+4a_2\frac{r^2}{R_b^2}\right\}\quad , \tag{67}$$

where $\Theta(x)$ is the Heaviside step function defined in Eq. (41). Making use of $\psi(r)=A(1+a_1r^2/R_b^2+a_2r^4/R_b^4)$ in Eq. (65), we obtain the body-wave dispersion relation

$$D_2(\omega)=\frac{\omega_{pb}^2}{\gamma_b^2[\omega^2-(\omega_b^+-\omega_b^-)^2]}\left[1+\frac{18\Omega_b^2}{\omega^2-4(\omega_b^+-\omega_b^-)^2}\right]=1\quad . \tag{68}$$

Moreover, it is also found that

$$a_1=\frac{\omega_{pb}^2}{\gamma_b^2[\omega^2-(\omega_b^+-\omega_b^-)^2]}\left\{a_1-\frac{24a_2\Omega_b^2}{\omega^2-4(\omega_b^+-\omega_b^-)^2}\right\}\quad , \tag{69}$$

which, when combined with Eq. (68), determines the relation between the

coefficients a_1 and a_2. After some straightforward algebra, it is found that

$$a_2=-(3/4)a_1 , \tag{70}$$

for $\ell=0$.

In order to determine the coefficient a_1, we eliminate the eigenfrequency ω and the coefficient a_2 from Eq. (67) by making use of Eqs. (68) and (70). Then, the eigenvalue equation in Eq. (67) can be simplified to give

$$\frac{1}{r}\frac{\partial}{\partial r} r \frac{\partial}{\partial r} \psi(r)=A \frac{a_1}{R_b} \delta(r-R_b)+4Aa_1 \frac{\Theta(R_b-r)}{R_b^2}\left(1-3\frac{r^2}{R_b^2}\right) . \tag{71}$$

Note from Eq. (71) that the perturbed surface-charge contribution [the term proportional to $\delta(r-R_b)$ in Eq. (71)] is not necessarily zero for perturbations with $(\ell,n)=(0,2)$. The physically acceptable solution to Eq. (71) is

$$\psi(r)=A\begin{cases} 1+a_1(r/R_b)^2(1-3r^2/4R_b^2), & 0 \le r < R_b , \\ (1+a_1/4)\ell n(r/R_c)/\ell n(R_b/R_c), & R_b < r \le R_c . \end{cases} \tag{72}$$

Multiplying Eq. (71) by r, integrating the resulting equation from $R_b(1-\epsilon)$ to $R_b(1+\epsilon)$ with $\epsilon\to 0_+$, and making use of Eq. (72), it is straightforward to show that

$$a_1=-4 \tag{73}$$

for perturbations with $(\ell,n)=(0,2)$. It is important to note from Eqs. (72) and (73) that the effective perturbed potential $\psi(r)$ is identically zero outside the beam ($R_b < r \le R_c$).

The dispersion relation in Eq. (68) can be expressed as

$$[\omega^2-(\omega_b^+-\omega_b^-)^2][\omega^2-4(\omega_b^+-\omega_b^-)^2]=\frac{\omega_{pb}^2}{\gamma_b^2}[\omega^2-4(\omega_b^+-\omega_b^-)^2+18\Omega_b^2] , \tag{74}$$

where $\Omega_b^2=(\omega_b^+-\omega_b)(\omega_b-\omega_b^-)$. Since the rotational frequency ω_b is a function of the thermal Larmor radius r_L [Eq. (22)], it is obvious from Eq. (74) that thermal Larmor radius effects play a significant role in determining stability behavior. As a particular case, it is instructive to examine the dispersion relation in Eq. (74) for a specified value of r_L corresponding to the maximum allowable beam density, i.e., $2(\omega_{pb}/\gamma_b\omega_{cb})^2=1-(2r_L/R_b)^2$ [see Eq. (23)]. In this case, the beam rotation frequency is given by $\omega_b=0.5\ \omega_{cb}$ [Eq. (22)], and the dispersion relation in Eq. (74) reduces to

$$[\omega^2-(\omega_b^+-\omega_b^-)^2][\omega^2-4(\omega_b^+-\omega_b^-)^2]=(\omega_{pb}^2/\gamma_b^2)[\omega^2+(\omega_b^+-\omega_b^-)^2/2], \qquad (75)$$

which is similar in form to the result obtained by Gluckstern[8] for perturbations about the Kapchinsky-Vladimirsky equilibrium distribution function in a quadrupole magnetic field.

Equation (76) is a simple quadratic equation for ω^2, and the necessary and sufficient condition for instability can be expressed as

$$\frac{\Omega_b^2}{(\omega_b^+-\omega_b^-)^2} > \frac{2}{9}\left[\left(\frac{\gamma_b\omega_{cb}}{\omega_{pb}}\right)^2-1\right] . \qquad (76)$$

Note that when Eq. (76) is satisfied, the perturbations are purely growing, i.e.,

$$\omega_r=\mathrm{Re}\omega=0 .$$

Several points are noteworthy from Eq. (76). First, thermal Larmor radius effects can have a large influence on stability behavior, since the parameter $\Omega_b^2=(\omega_b^+-\omega_b)(\omega_b-\omega_b^-)$ in Eq. (76) is a function of r_L [Eq. (22)]. Second, for the case of cold laminar flow characterized by $r_L=0$ and $\omega_b=\omega_b^{\pm}$, perturbations with mode numbers $(\ell,n)=(0,2)$ do not exhibit instability, because $\Omega_b^2=0$ in this limit. Finally, we note from Eqs. (13), (14), (22), and (76) that for specified value of thermal Larmor radius r_L, the stability behavior is identical for both fast (+) and slow (-)

rotational equilibria defined in Eq. (22).

The stability boundary in the parameter space $(r_L/R_b,\ \omega_{pb}^2/\gamma_b^2\omega_{cb}^2)$ is determined from Eq. (76). A numerical investigation of Eq. (76) indicates that the stability boundary is almost identical to the equilibrium boundary given in Eq. (23) and Fig. 2. In this regard, we conclude that there is only a very narrow region of $(r_L/R_b,\ \omega_{pb}^2/\gamma_b^2\omega_{cb}^2)$ parameter space that corresponds to instability for perturbations with $(\ell,n)=(0,2)$. In particular, the equilibrium boundary $2(\omega_{pb}/\gamma_b\omega_{cb})^2=1-(2r_L/R_b)^2$, which corresponds to $\omega_b=0.5\ \omega_{cb}$, exhibits instability.

It is instructive to investigate stability properties on the equilibrium boundary characterized by $\omega_b=0.5\ \omega_{cb}$, which corresponds to the maximum beam density for a given value of thermal Larmor radius r_L. Making use of $2(\omega_{pb}/\gamma_b\omega_{cb})^2=1-(2r_L/R_b)^2$ and defining the effective beam luminosity σ by

$$\sigma=(\omega_{pb}R_b/2\gamma_b\omega_{cb}r_L)^2\ , \tag{77}$$

it is straightforward to express Eq. (76) and the inequality $2(\omega_{pb}/\gamma_b\omega_{cb})^2<1$ as

$$8<\sigma<\infty\ , \tag{78}$$

which is the necessary and sufficient condition for instability for $\omega_b=0.5\ \omega_{cb}$. Figure 5 shows a plot of the normalized growth rate $\mathrm{Im}\omega/\omega_{cb}$ versus the effective beam luminosity σ obtained from Eq. (75) for $\omega_b=0.5\ \omega_{cb}$. As shown in Eq. (78), we also note from Fig. 5 that instability exists only for σ in the range $8<\sigma<\infty$. The instability growth rate increases rapidly from zero (at $\sigma=8$) to its maximum value $0.076\ \omega_{cb}$ (at $\sigma=20$) and then decreases slowly to zero as the effective beam luminosity is increased from $\sigma=8$ to infinity.

In this section, we have investigated stability properties of a

relativistic electron beam in a uniform axial magnetic field for perturbations with infinitely long axial wavelength. Several points are noteworthy in these studies. First, surface-wave perturbations, characterized by the eigenfunction $\psi(r)=Ar^{\ell}$ inside the beam, do not exhibit instability (Sec. IV.A). Second, perturbations with radial mode number n=1 have been studied in Sec. IV.B, and the dispersion relation has been derived for arbitrary value of azimuthal mode number ℓ. It is found that perturbations with ℓ=0, 1, and 2 do not exhibit instability for the entire allowed range of equilibrium density and thermal Larmor radius. Third, the stability analysis for azimuthally symmetric perturbations (ℓ=0) and radial mode number n=2 has been carried out in Sec. IV.C. Instability is found for $\omega_b = 0.5\ \omega_{cb}$. The physical mechanism of instability has been explained by Hofmann[16] in terms of negative energy wave in an intense beam. However, the system can be easily stabilized by slightly detuning the rotational frequency from $\omega_b=0.5\ \omega_{cb}$.

In summary, we conclude that perturbations with low radial and azimuthal mode numbers are either stable or easily stabilized for the allowed range of equilibrium parameters in Fig. 2. Stability properties for high-mode-number perturbations are presently under investigation.

V. INFLUENCE OF BEAM ROTATION ON THE TRANSVERSE INSTABILITY OF AN ION BEAM IN A QUADRUPOLE MAGNETIC FIELD

Recent studies[10] have examined the feasibility of using intense heavy ion beams as the source of ignition energy for inertially confined fusion reactions. In this regard, it appears that heavy ion beams with suitable energies and densities can be used as viable drivers. One of the major limitations on beam transport may be due to the transverse instability[8,9] that originates from beam self-field effects. In this context, it is important to examine the transverse instability[8,9] for an ion beam in a quadrupole magnetic field. Several theoretical and experimental studies of this instability are being carried out.[11-14] In this section, we investigate the influence of ion beam rotational frequency on stability behavior, making use of the theoretical formalism developed in Sec. IV of this paper.

In order to simplify the analysis, we consider ion motion in the average external magnetic field[8] provided by periodic quadrupole magnets. In this regard, the focussing for a associated with the applied quadrupole field can be determined from the axial component of the effective vector potential

$$A_z^{ext}(r)=-(\gamma_b m/2e\beta_b)\omega_f^2 r^2 \quad , \tag{79}$$

where the oscillation frequency ω_f is related to the quadrupole field gradient,[8] and e and m are the ion charge and rest mass, respectively. In a conventional particle accelerator, there is no applied axial magnetic field. However, to make the analysis in this section more general, we do allow for a nonzero axial magnetic field $B_0\hat{e}_z$.

Making use of Eq. (79), it is straightforward to express the three single-particle constants of motion in Eq. (3) as the energy

$$H=(m^2c^4+c^2p_\zeta^2)^{1/2}+e\phi_0(r), \tag{80}$$

the canonical angular momentum

$$P_\theta=(rp_\theta+eB_0r^2/2c) , \tag{81}$$

and the axial canonical momentum

$$P_z=p_z-(\gamma_b m/2\beta_b c)\omega_f^2 r^2+(e/c)A_0(r) , \tag{82}$$

where $A_0(r)$ is the axial component of vector potential for the equilibrium azimuthal self-magnetic field. In the subsequent analysis, it is useful to note from Eqs. (3) and (81) that, in the limit where $\omega_b=0$ and $B_0=0$, the beam distribution function in Eq. (3) is identical to the Kapchinsky-Vladimirsky distribution function.

The equilibrium potentials $\phi_0(r)$ and $A_0(r)$ in Eqs. (80) and (82) are calculated self-consistently from the steady-state Maxwell equations

$$\frac{1}{r}\frac{\partial}{\partial r}\, r\, \frac{\partial}{\partial r}\, \phi_0(r)=-4\pi e n_b^0(r) , \tag{83}$$

and

$$\frac{1}{r}\frac{\partial}{\partial r}\, r\, \frac{\partial}{\partial r}\, A_0(r)=-\frac{4\pi e}{c}\, n_b^0(r)V_z^0(r) . \tag{84}$$

Making use of Eqs. (80)-(84), it is straightforward to show that beam equilibrium properties are identical to the results obtained in Sec. II, if we replace electrons by ions and redefine Ω_b^2 [Eq. (13)] to include the influence of the quadrupole field, i.e.,

$$\Omega_b^2=(\omega_b^+-\omega_b)(\omega_b-\omega_b^-)$$

$$=-\omega_b\omega_{cb}-\omega_b^2+\omega_f^2-\omega_{pb}^2/2\gamma_b^2 . \tag{85}$$

In Eq. (85), the laminar rotation frequency $\omega_b^\pm$ is defined by

$$\omega_b^{\pm}=-\frac{1}{2}\left(\omega_{cb}\pm\left(\omega_{cb}^2+4\omega_f^2-\frac{2\omega_{pb}^2}{\gamma_b^2}\right)^{1/2}\right) , \tag{86}$$

where $\omega_{cb}=eB_0/\gamma_b mc$ is the ion cyclotron frequency.

Expressing the beam rotation frequency in terms of the transverse temperature $\hat{T}_\perp=\gamma_b m\omega_{cb}^2 r_L^2/2$ [Eq. (20)], we obtain

$$\omega_b=\hat{\omega}_b^{\pm}=-\frac{1}{2}\left(\omega_{cb}\pm\left(\omega_{cb}^2+4\omega_f^2-\frac{2\omega_{pb}^2}{\gamma_b^2}-\frac{8\hat{T}_\perp}{\gamma_b mR_b^2}\right)^{1/2}\right) . \tag{87}$$

For equilibrium to exist, the ion beam density is bounded by

$$\frac{\omega_{pb}^2}{\gamma_b^2} \leq 2\omega_f^2+\frac{1}{2}\omega_{cb}^2-\frac{4\hat{T}_\perp}{\gamma_b mR_b^2} . \tag{88}$$

One of the important features of Eq. (88) is that, for specified values of ω_f and $T_\perp$, the limiting beam density can be substantially increased by increasing the applied axial magnetic field. The reason is simply that the axial magnetic field provides a radially confining force in addition to the quadrupole magnetic field.

According to the analysis in Sec. IV, the possibility of instability exists for azimuthally symmetric ($\ell=0$) perturbations with radial mode number n=2. For this particular mode, the dispersion relation is given by Eq. (74) (replacing electrons by ions), where the laminar rotation frequencies are defined in Eq. (86). Our primary interest in this section is to determine the influence of rotation frequency ω_b on stability behavior. For simplicity, we therefore consider the case of zero applied axial field ($B_0=0$). Equations (86) and (87) can be expressed as

$$\omega_b^{\pm}=\mp\hat{\omega}_b , \quad \omega_b=\mp\left(\hat{\omega}_b^2-\frac{2T_\perp}{\gamma_b mR_b^2}\right)^{1/2} , \tag{89}$$

where $\hat{\omega}_b$ is defined by

$$\hat{\omega}_b=(\omega_f^2-\omega_{pb}^2/2\gamma_b^2)^{1/2} . \tag{90}$$

As a check on the dispersion relation given in Eq. (74), we examine the limiting case characterized by $\omega_b=0$ and $\hat{\omega}_b^2=2T_\perp/\gamma_b mR_b^2$. For this special choice of parameters, the dispersion relation in Eq. (74) can be expressed as

$$(\omega^2-4\hat{\omega}_b^2)(\omega^2-16\hat{\omega}_b^2)=(\omega_{pb}^2/\gamma_b^2)(\omega^2+2\hat{\omega}_b^2) \quad , \tag{91}$$

which is identical to the result obtained by Gluckstern.[8] Instability readily follows from Eq. (91). This instability has also been observed in computer simulations by Haber[9] for the case $\omega_b=0$.

For zero axial magnetic field ($B_0=0$), and general value of rotation frequency ω_b consistent with Eq. (89), it is straightforward to show from Eqs. (74) and (89) that the necessary and sufficient condition for instability is given by

$$\frac{\gamma_b^2\omega_b^2}{\omega_{pb}^2} < h(\omega_f^2\gamma_b^2/\omega_{pb}^2) \quad , \tag{92}$$

where h(x) is defined by

$$h(x)= \frac{1}{9}\,(x-\frac{1}{2})(17-32x) \quad . \tag{93}$$

Evidently, the function h(x) assumes its maximum value, $h_m=1/1152$, at $x=33/64$. As shown in Eq. (92), the beam rotation (ω_b) plays a critical role in determining stability behavior. Moreover, perturbations with mode numbers $(\ell,n)=(0,2)$ can be completely stabilized by increasing the rotation frequency to values satisfying

$$(\gamma_b\omega_b/\omega_{pb})^2 > h_m=1/1152. \tag{94}$$

Finally, we conclude by summarizing several important results obtained in this section. First, in the equilibrium analysis, it is found that the maximum allowable beam density can be significantly

increased by increasing the axial magnetic field B_0 [Eq. (88)]. Second, for perturbations with $(\ell,n)=(0,2)$, we recover the previous stability results obtained by Gluckstern[9] for $\omega_b=0$ and $B_0=0$. Third, the value of rotational frequency ω_b is found to play a significant role in determining stability properties [Eqs. (92) and (94)]. Finally, for general value of B_0, the maximum instability occurs for $\omega_b=-0.5\,\omega_{cb}$. Since the distribution function in Eq. (3) is very similar to the Kapchinsky-Vladimivsky distribution function in the Larmor frame characterized by $\omega_b=-0.5\,\omega_{cb}$, the instability mechanism for $(\ell,n) = (0,2)$ is identical to that of the breathing mode first found by Gluckstern[8]. However, for azimuthally symmetric perturbations with $\ell=0$ and $n=2$, the system can be easily stabilized by slightly detuning the rotational frequency from the value $\omega_b=-0.5\,\omega_{cb}$.

VI. CONCLUSIONS

In this paper we have investigated the stability properties for low-frequency flute perturbations in a relativistic nonneutral electron beam propagating parallel to a uniform axial magnetic field $B_0\hat{e}_z$. The analysis was carried out within the framework of the Vlasov-Maxwell equations, assuming that all perturbed quantities are independent of axial coordinate ($\partial/\partial z=0$). In Sec. II, equilibrium properties were calculated for the choice of rigid-rotor distribution function in which all electrons have the same value of axial canonical momentum and the same value of energy in a frame of reference rotating with angular velocity ω_b. The linearized Vlasov-Maxwell equations were examined in Sec. III, and the stability properties for low-frequency flute perturbations characterized by $|\omega R_b| << \ell c$ were investigated in Sec. IV, including the important influence of electron thermal Larmor radius effects on stability behavior. Several points are noteworthy in the stability studies. First, for n=0 and all values of ℓ, surface-wave perturbations do not exhibit instability for any allowed values of equilibrium parameters. Second, the same conclusion holds for body-wave perturbations with $(\ell,n)=(0,1)$, $(1,1)$, and $(2,1)$. Third, the stability analysis for body-wave perturbations with $(\ell,n)=(0,2)$ was carried out in Sec. IV.C. Instability is found for the special choice of beam rotation frequency $\omega_b=0.5\ \omega_{cb}$. However, this mode can be easily stabilized by slightly detuning the rotational frequency from the value $\omega_b=0.5\ \omega_{cb}$.

As a further application of the stability formalism developed in Secs. II-IV, in Sec. V we investigated the influence of beam rotation on the transverse instability for an intense ion beam in a quadrupole magnetic field. In this case, it is also found that beam rotation plays an important role in determining detailed stability properties.

Moreover, the instability can be easily stabilized by an appropriate change in rotation frequency ω_b. Finally, we emphasize that the present stability analysis has emphasized perturbations with low radial and azimuthal mode numbers. Stability properties for perturbations with high mode numbers are presently under investigation.

ACKNOWLEDGMENTS

It is a pleasure to acknowledge the benefit of useful discussions with Dr. Won Namkung.

This research was supported in part by the Independent Research Fund at the Naval Surface Weapons Center and in part by the Office of Naval Research.

REFERENCES

1. R. C. Davidson and H. S. Uhm, Phys. Fluids 22, 1375 (1979).
2. M. Reiser, Phys. Fluids 20, 477 (1977).
3. H. S. Uhm and R. C. Davidson, Phys. Fluids, 23, in press (1980).
4. H. S. Uhm and R. C. Davidson, J. Appl. Phys. 50, 696 (1979).
5. M. L. Sloan and W. E. Drummond, Phys. Rev. Lett. 31, 1234 (1973).
6. P. Sprangle, A. Drobot, and W. Manheimer, Phys. Rev. Lett. 36, 1180 (1976).
7. W. W. Destler, H. S. Uhm, H. Kim, and M. P. Reiser, J. Appl. Phys. 50, 3015 (1979).
8. R.L. Gluckstern, Proc. 1970 Proton Linac Conf. edited by M.R. Tracy, (National Accel. Lab., Batavia, ILL., 1970) p. 811.
9. I. Haber and A.W. Maschke, Phys. Rev. Lett. 42, 1479 (1979).
10. T.F. Godlove, IEEE Trans. Nucl. Sci. NS-26, 2997 (1979).
11. M. Reiser, W. Namkung, and M. A. Brennan, IEEE Trans. Nucl. Sci. NS-26, 3026 (1979).
12. L. J. Laslett and L. Smith, IEEE Trans. Nucl. Sci. NS-26, 3080 (1979).
13. S. Abbott, W. Chupp, A. Faltens, W. Herrmannsfeldt, E. Hoyer, D. Keefe, C. H. Kim, S. Rosenblum, and J. Shiloh, IEEE Trans. Nucl. Sci. NS-26, 3095 (1979).
14. M. G. Mazarakis, R. J. Burke, E. P. Colton, S. Fenster, J. S. Moenich, D. K. Nikfarjam, D. W. Price, N. Q. Sesol, and J. M. Watson, IEEE Trans. Nucl. Sci. NS-26, 3042 (1979).
15. I. M. Kapchinsky and V. V. Vladimirsky, Proc. Int. Conf. on High Energy Accelerators, and Instrumentation, edited by L. Kowarski, (Cern, Geneva, 1959), p. 24.
16. I. Hofmann, "Negative Energy Oscillations and Instability of Intense Beams", D-8046 Garching/FRG, Max-Planck-Institut für Plasmaphysik; also submitted to Particle Accelerators.

FIGURE CAPTIONS

Fig. 1 Equilibrium configuration and coordinate system.

Fig. 2 Allowed equilibria [Eq. (23)].

Fig. 3 Plot of rotational frequency ω_b/ω_{cb} versus $2\omega_{pb}^2/\gamma_b^2\omega_{cb}^2+(2r_L/R_b)^2$ [Eq. (22)].

Fig. 4 Plots of $D_1(\omega)$ versus ω [Eqs. (55) and (63)] for the range of ω_b satisfying (a) $\omega_b^+ + 2\omega_b^- > 3\omega_b$, (b) $2\omega_b^+ + \omega_b^- > 3\omega_b > \omega_b^+ + 2\omega_b^-$, and (c) $3\omega_b > 2\omega_b^+ + \omega_b^-$.

Fig. 5 Plot of normalized growth rate $\mathrm{Im}\omega/\omega_{cb}$ versus the effective beam luminosity σ [Eq. (25)] for $\omega_b = 0.5\ \omega_{cb}$.

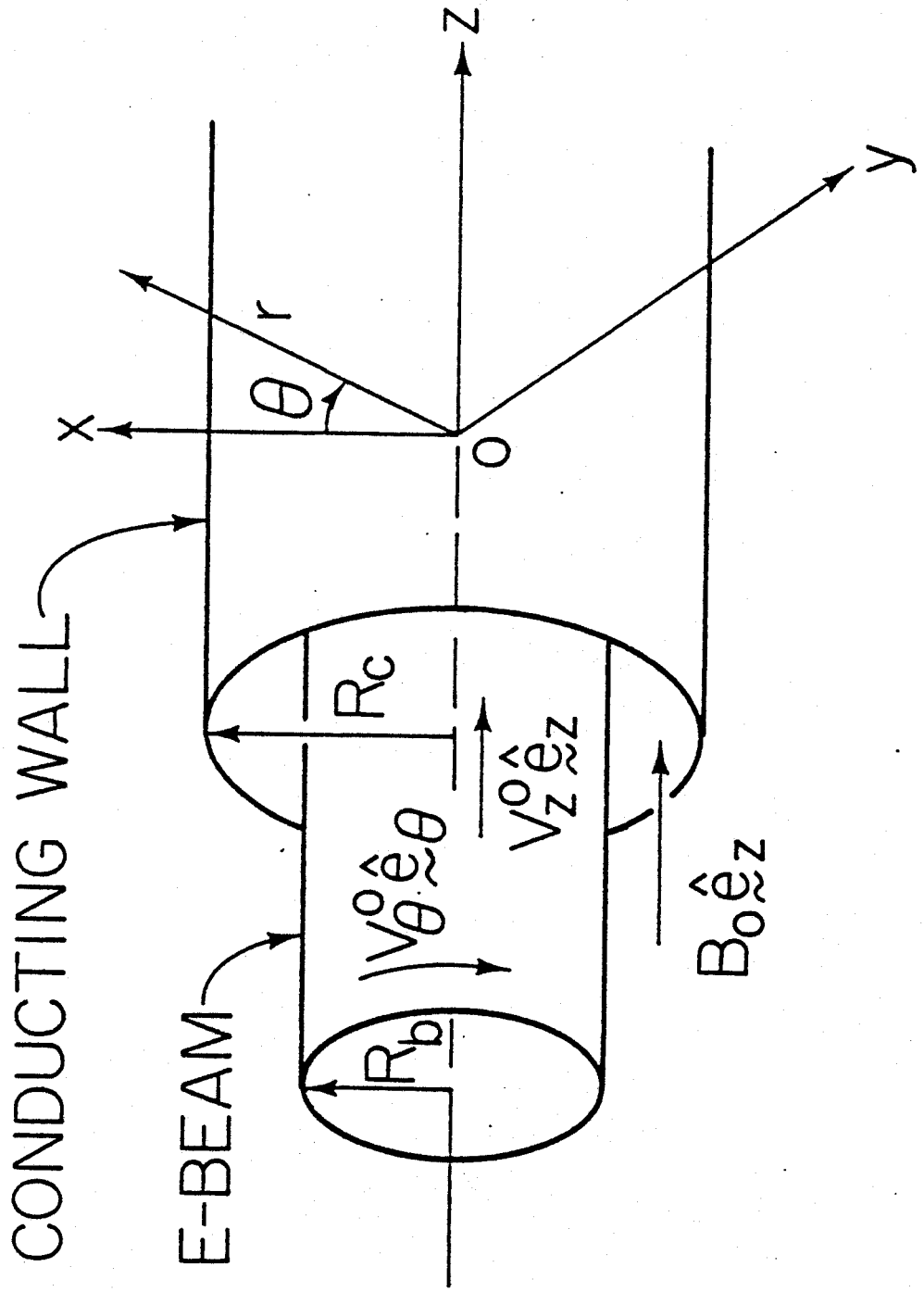
z
y
r
θ
x
O
CONDUCTING WALL
E-BEAM
R_c
R_b
$V_\theta^o \hat{e}_\theta$
$V_z^o \hat{e}_z$
$B_o \hat{e}_z$

Fig. 1

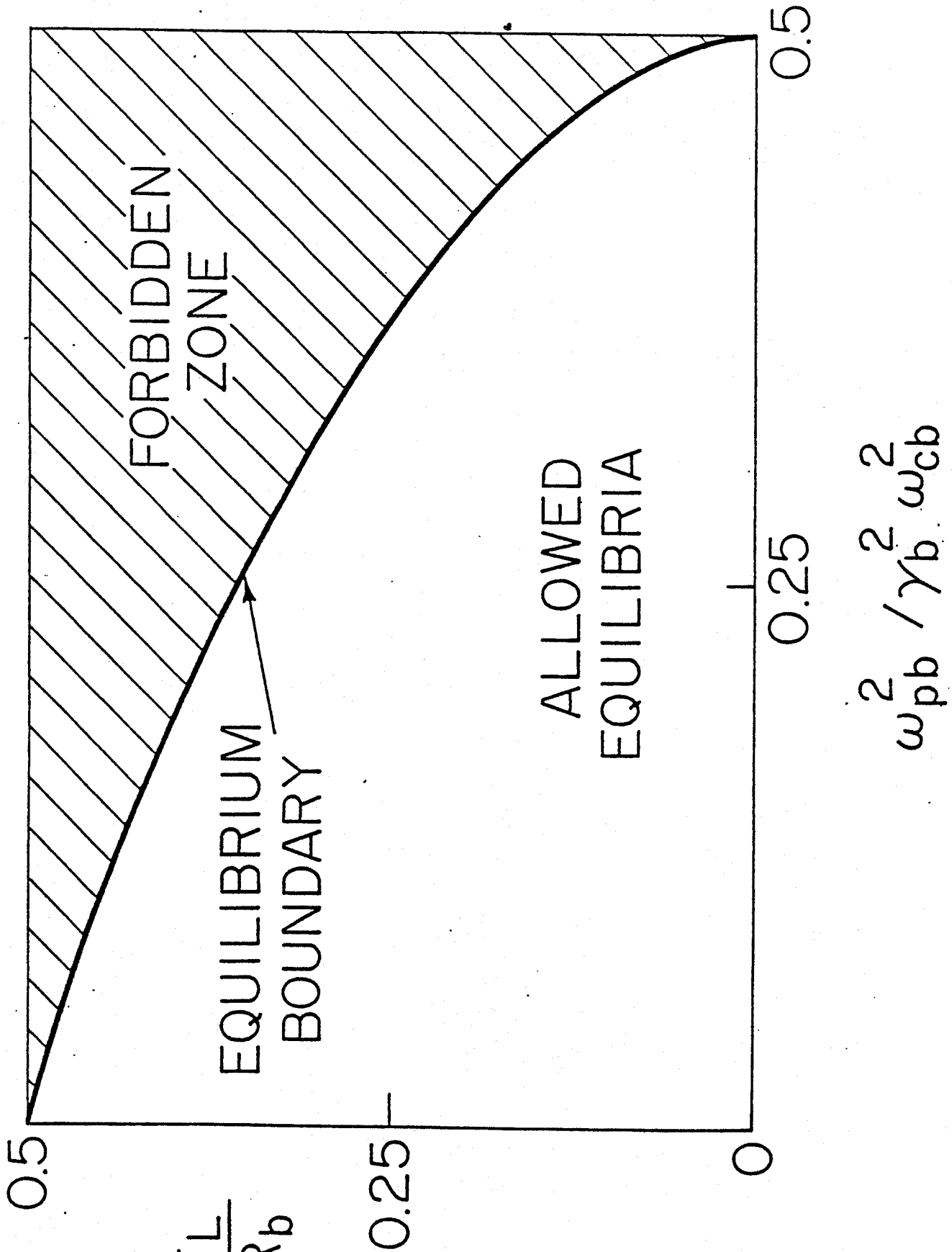
FORBIDDEN ZONE
EQUILIBRIUM BOUNDARY
ALLOWED EQUILIBRIA
0.5
0.25
0
0.5
0.25
$\frac{r_L}{R_b}$
$\omega_{pb}^2 / \gamma_b^2 \omega_{cb}^2$

Fig. 2

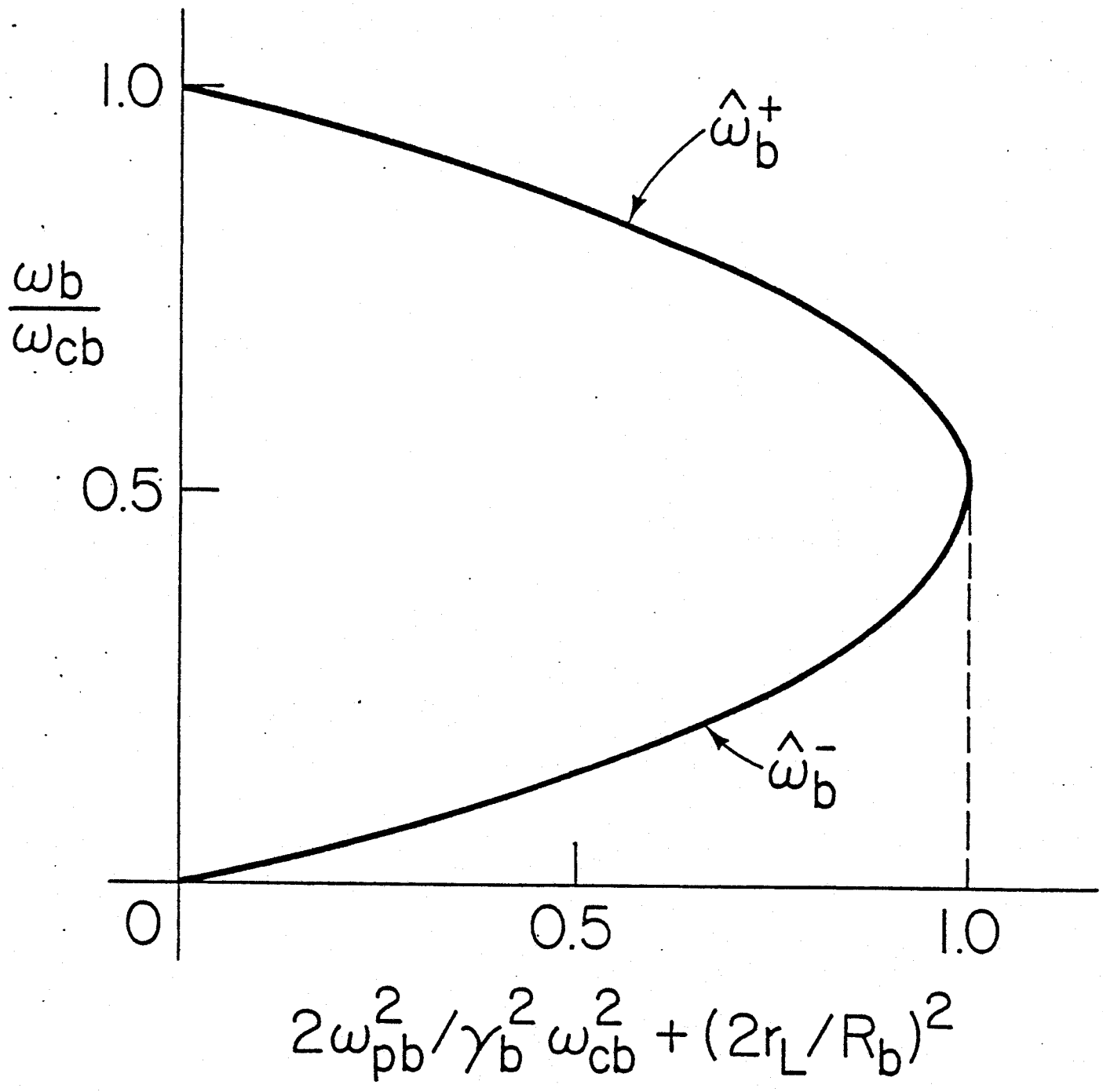
1.0
0.5
0
$\frac{\omega_b}{\omega_{cb}}$
$\hat{\omega}_b^+$
$\hat{\omega}_b^-$
0.5
1.0
$2\omega_{pb}^2/\gamma_b^2\omega_{cb}^2 + (2r_L/R_b)^2$

Fig. 3

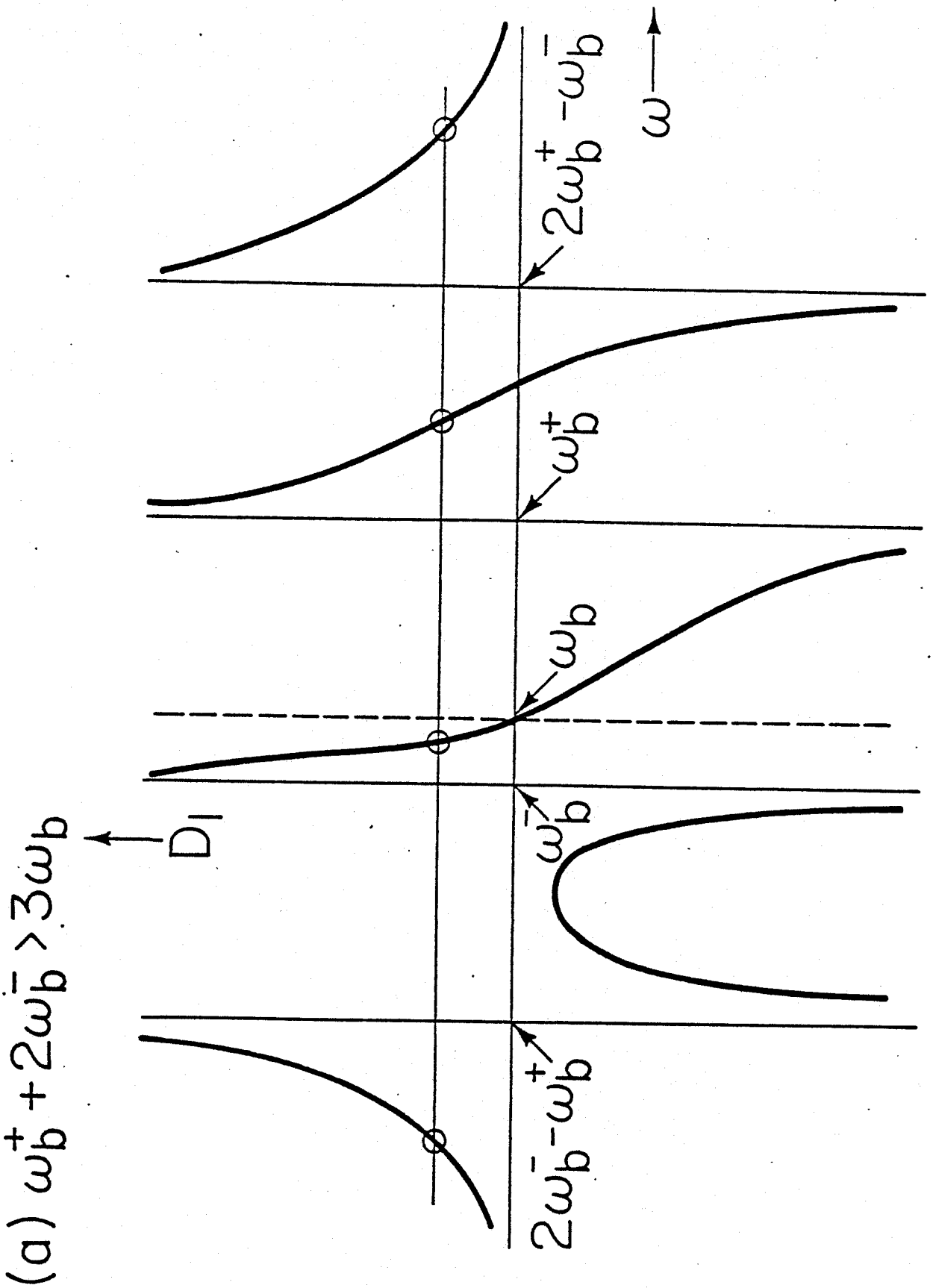
(a) $\omega_b^+ + 2\omega_b^- > 3\omega_b$
D_I
ω
$2\omega_b^+ - \omega_b^-$
ω_b^+
ω_b
ω_b^-
$2\omega_b^- - \omega_b^+$

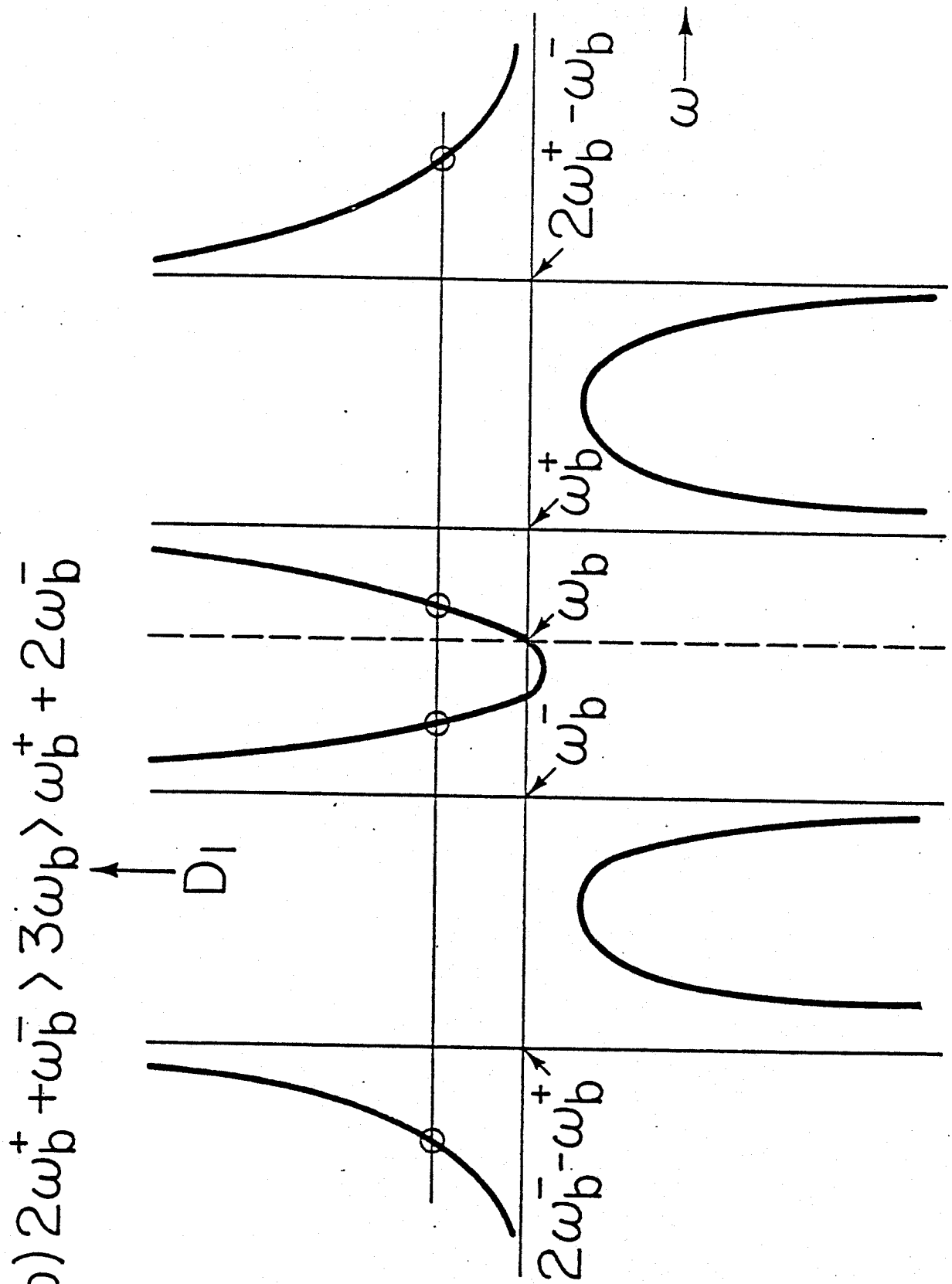
(b) $2\omega_b^+ + \omega_b^- > 3\omega_b > \omega_b^+ + 2\omega_b^-$
D_I
$2\omega_b^+ - \omega_b^-$
ω_b^+
ω_b
ω_b^-
$2\omega_b^- - \omega_b^+$
ω

Fig. 4(b)

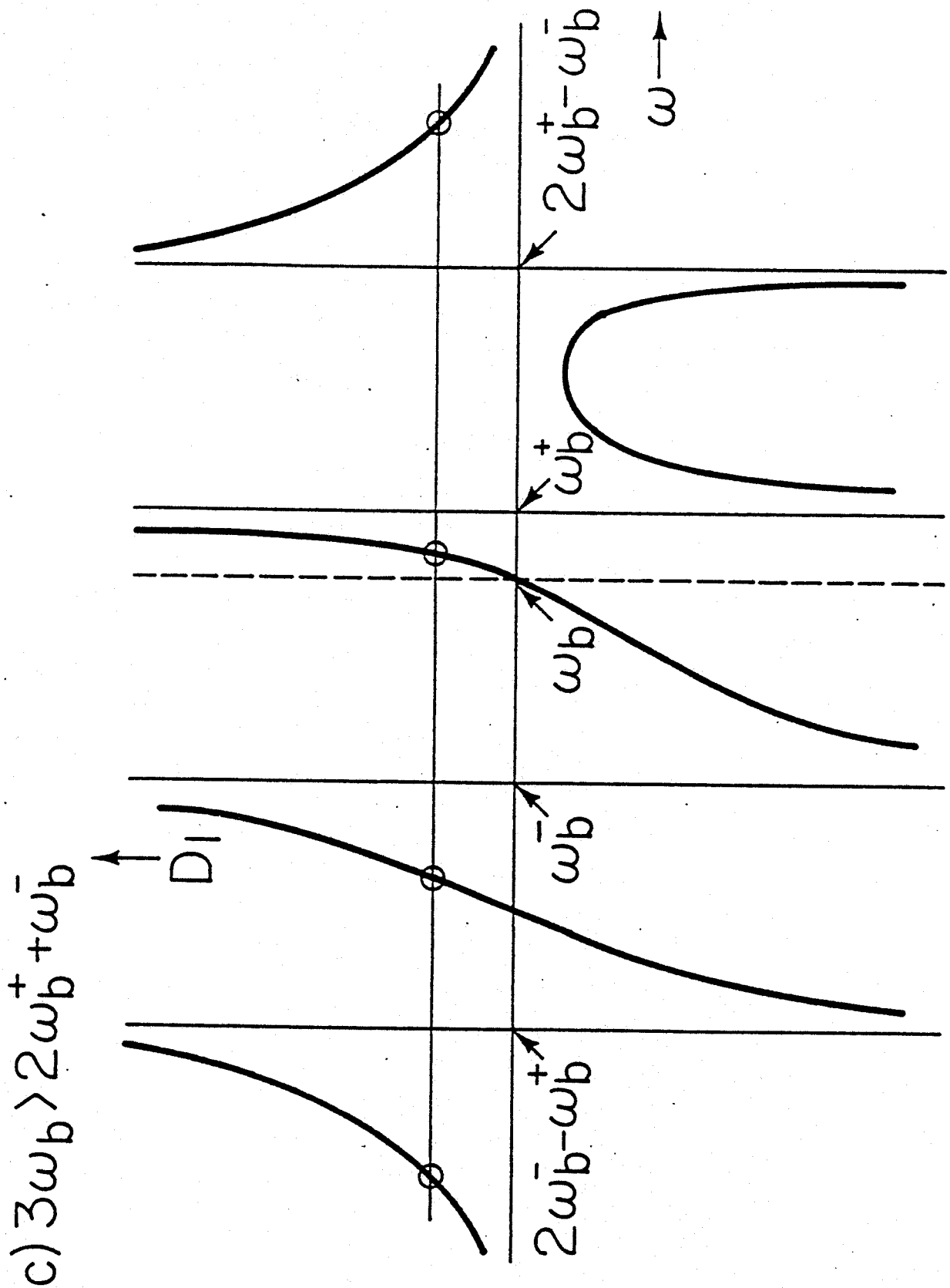
(c) $3\omega_b > 2\omega_b^+ + \omega_b^-$
D_I
ω_b^-
ω_b
ω_b^+
$2\omega_b^+ - \omega_b^-$
$2\omega_b^- - \omega_b^+$
$\omega \longrightarrow$

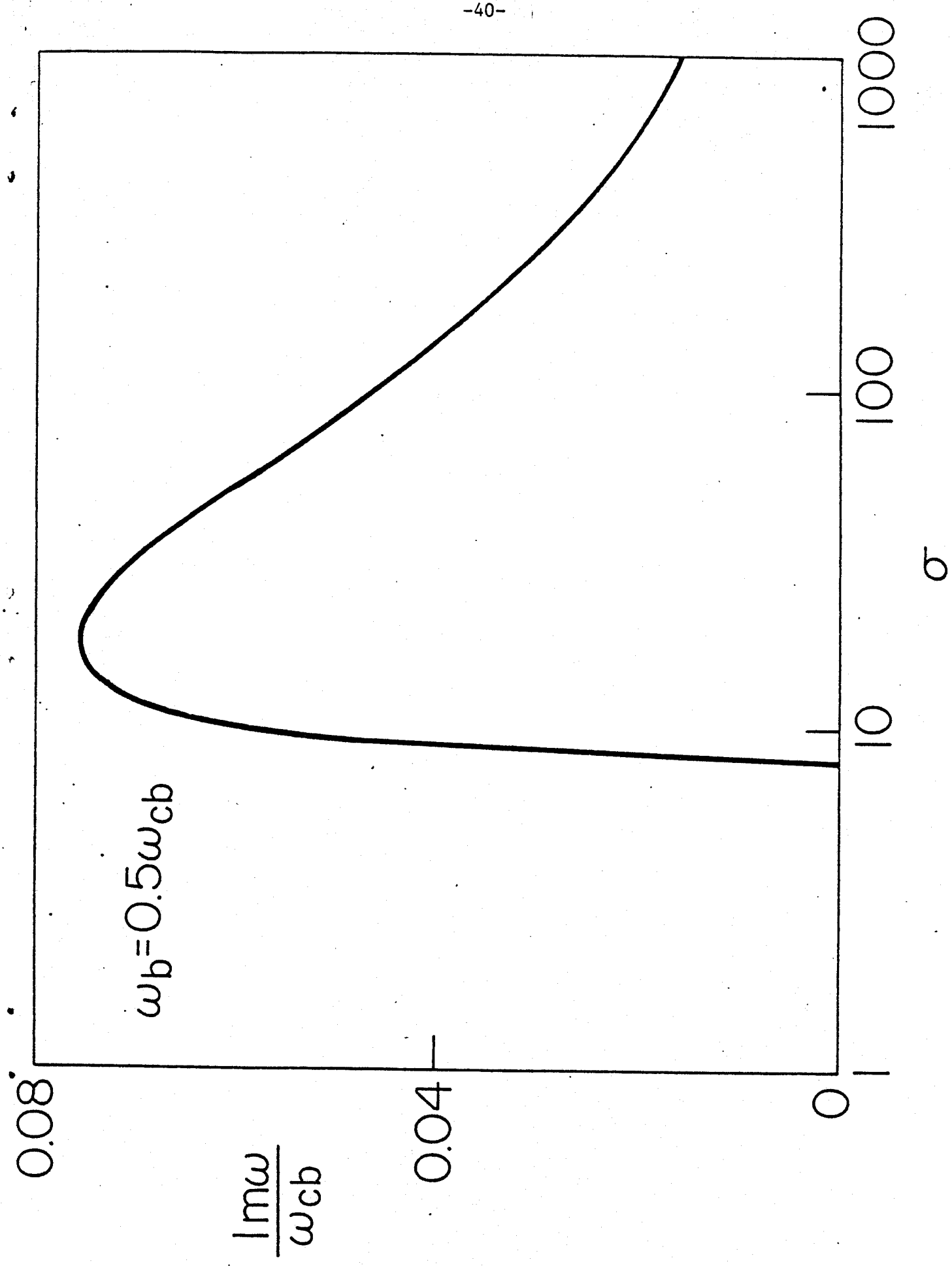
0.08
0.04
0
$\frac{Im\omega}{\omega_{cb}}$
$\omega_b=0.5\omega_{cb}$
1
10
100
1000
σ

Fig. 5